DRAFT
CMS Physics Analysis Summary

2010/02/25
Head Id: 3351
Archive Id:
Archive Date: 2010/02/23
Archive Tag: trunk

$\pi^{\pm}\pi^{\pm}$

Measurement of Bose–Einstein Correlations in 0.9 and 2.36 TeV proton-proton Collisions with the CMS Detector

The CMS Collaboration

Abstract

This document describes the extraction of a signal of Bose–Einstein correlations of charged hadron candidates from the first sample of 0.9 and 2.36 TeV proton-proton collisions recorded by the CMS detector in December 2009.
The signal is observed in the form of an enhancement of pairs of same-sign charged particles with very small relative momentum, with respect to an appropriate reference sample. By parametrizing the effect with a simple exponential form, the average size of the correlated emission region is estimated to be $r = 1.62 \pm 0.05$ (stat) ± 0.27(syst) fm ($r = 1.96 \pm 0.20$ (stat) ± 0.27 (syst) fm) and the intensity of the effect is estimated to be $\lambda = 0.634 \pm 0.021$ (stat) ± 0.047 (syst) ($\lambda = 0.68 \pm 0.11$ (stat) ± 0.05 (syst)) in 0.9 TeV (2.36 TeV) collisions, respectively.

1 Introduction

This document summarizes the first measurement of a Bose–Einstein correlation signal (BEC) from charged hadron candidates collected by the CMS detector in 0.9 and 2.36 TeV proton-proton collisions collected by the Large Hadron Collider in December 2009. A detailed description of the CMS detector is available in [1].

The spin-statistics correlation among identical bosons can be studied in elementary particle collisions by observing an enhancement of pairs or multiplets of such particles in the region of phase space where their momenta are very similar. Measurements of the interference resulting from the Bose–Einstein symmetrization of the multi-particle wave function give access to a determination of the space-time structure of the region of emission of the bosons.

The first demonstration of Bose–Einstein correlations in pion production was obtained fifty years ago by Goldhaber and collaborators in proton-antiproton interactions [2]. A number of measurements, using a variety of initial states, has been produced by different experiments since then: MARKII [3], TASSO [4], ALEPH [5], DELPHI [6], OPAL [7], NA22 [8], ZEUS [9], UA1 [10]. These experiments measured the magnitude of the effect, the size of the emission region where a constructive interference is observed, and the dependence of these attributes on other characteristics of the collisions.

The typical means by which the interference is studied is via a ratio R between the joint probability that a pair of identical bosons are emitted, $P(p_1, p_2)$, and the product of the single-particle probabilities $P(p_1)P(p_2)$,

$$R = \frac{P(p_1, p_2)}{P(p_1)P(p_2)}, \tag{1}$$

where probabilities P are expressed as a function of the particles four-momenta p_1 and p_2.

In practice R is measured as a function of a single quantity, combining the four-momenta of the two particles. Among the various variables proposed in the literature, we choose the Lorentz-invariant four-momentum transfer, $Q = \sqrt{-(p_1 - p_2)^2}$ or $Q = \sqrt{m_{inv}^2 - 4m_\pi^2}$, where m_{inv} is the combined invariant mass of the two particles (assumed to both have the charged pion mass, m_π). The ratio R may thus be derived experimentally by dividing the Q distribution of pairs of identical bosons by a reference sample constructed with pairs of tracks which have by construction no correlation among each other; however, such reference samples are not easy to construct, since in most instances they often present small, weak variations with Q from the behavior of the studied identical bosons. We discuss in detail the choice of a proper reference sample in Sec. 5.

The ratio R can be parameterized in several ways. A Lorentz-invariant representation widely used in the literature describes the emission from a spherical region parametrized by the following expression:

$$R(Q) = C[1 + \lambda\Omega(Qr)] \cdot (1 + \delta Q). \tag{2}$$

Here $\Omega(Qr)$ is the Fourier trasform of the emission region, characterized by an effective size r. Several different expressions have been used in the past: $\Omega(Qr) = e^{-Qr}$; $\Omega(Qr) = e^{-(Qr)^2}$; $\Omega(Qr) = 1/(1 + Qr)^2$; or $\Omega(Qr) = [J_1(Qr)/Qr)]^2$ (see [11] and references therein). The

strength parameter $\lambda < 1$ allows for measurements of a partial interference, which may arise because of the interaction between the produced bosons or because of other coherent-production mechanisms. The δ factor accounts for long-distance correlations or biases introduced by the use of non-ideal reference samples. C is a normalization factor.

Another analytical expression derived from quantum-field theory is detailed in [12]. The authors suggest the following form:

$$R(Q) = C[1 + \frac{2\alpha}{(1+\alpha)^2}\sqrt{\Omega(Qr)} + \frac{1}{(1+)^2}\Omega(Qr)](1+\delta Q). \quad (3)$$

2 Datasets and Preselection

We use experimental data collected in 0.9 TeV physics runs taken in December 2009. During the data-taking periods the beam was stable and the detector was fully operational. We find a total of 270,472 minimum-bias events triggered by the High-Level Trigger (HLT_MinBiasBSC) containing at least two and at most 150 charged tracks.

During December 2009 CMS also collected an additional set of events from two runs of 2.36 TeV proton-proton collisions, for a total of 13,548 events after the same selection described above. This sample is still sufficient for a measurement of Bose–Einstein correlations in these higher-energy collisions.

Together with experimental data, we analyze samples of minimum bias Monte Carlo events simulating 0.9 and 2.36 TeV proton-proton collisions. Each sample contains a total of 1,000,000 events. These simulations do not include a modeling of Bose–Einstein correlations among identical bosons. In the following, these samples will be addressed as "default simulation".

The Pythia Monte Carlo includes the functionality to simulate Bose–Einstein correlation effects, with a few caveats[13] which are not a concern as long as these samples are used as a simple cross-check of the sensitivity of the analysis. Following the suggestions of one of the authors [14], we generated two 1,000,000 sets of minimum-bias events with settings corresponding to a strength parameter $\lambda = 0.4$ and a coherence radius $r = 0.8$ fm. The two samples are generated with a Gaussian and an exponential functional form for the shape of the correlation function, respectively. All the other parameters are fixed to the values used in the standard simulation of minimum-bias events.

3 Selection of Track Pairs

The selection of charged tracks is based on the need of retaining tracks of good quality. The analysis focuses on low-momentum pions, for which the effect of a Bose–Einstein interference is known to be largest in particle collisions. We use charged tracks with $p_t > 200$ MeV/c, which is enough for promptly-produced particles to cross the third layer of the silicon pixel detector, and pseudorapidity $|\eta| < 2.4$ to ensure a full acceptance.

We select tracks of high purity having more than five degrees of freedom for the reconstruction fit, and a normalized $\chi^2 < 5.0$. We further require a transverse impact parameter with respect to the collision point $|d_{xy}| < 0.15$ cm, and the innermost measured point of the track at a radius $R < 20$ cm; these rather tight requirements are aimed at removing electrons and positrons produced from photon conversions in the detector material, and secondary particles originated from the decay of long-lived particles (K_s, Λ, etc.).

We provide below a table detailing the selection of track pairs which constitute our Bose–Einstein pion candidate sample in 0.9 and 2.36 TeV data.

Table 1: List of selection requirements applied to experimental data at 0.9 and 2.36 TeV, and corresponding statistics of tracks.

Selection	Events at 0.9 TeV	Accepted tracks	Events at 2.36 TeV	Accepted tracks
Preselection	270,472	5,374,254	13,548	343,880
$N_{dof} > 5$		3,673,132		238,879
$p_t > 200 MeV/c$		3,508,439		228,495
$\chi^2 < 5.0$		3,482,908		226,959
$\|\eta\| < 2.4$		3,385,375		220,506
$d_{xy} < 0.15 cm$		2,912,508		188,687
$R_{xy} < 20 cm$		2,903,754		188,140

The distribution of a few kinematical variables for the tracks before and after the above selection for 0.9 TeV experimental data and corresponding default simulation are shown in Fig. 1 and Fig. 2.

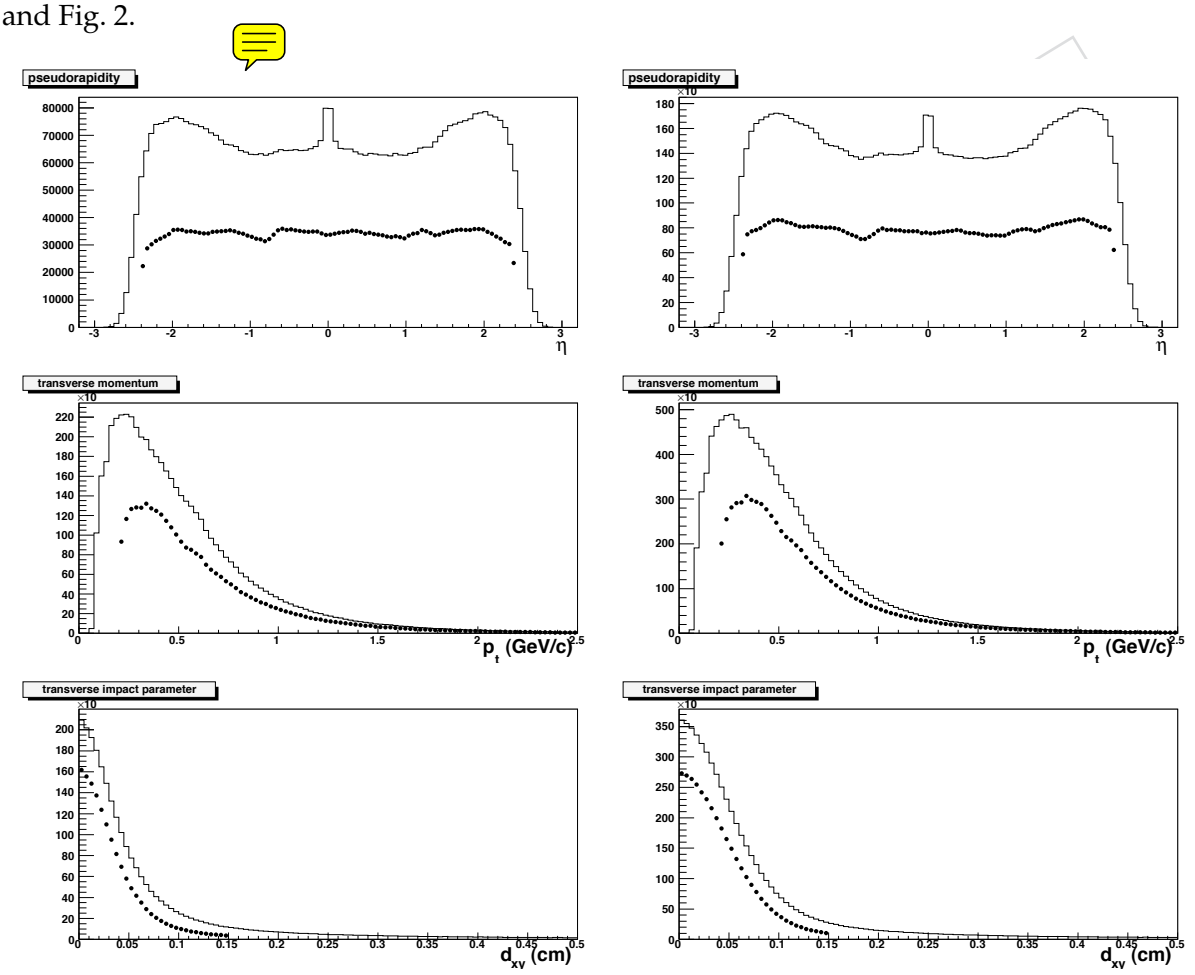

Figure 1: Events at $\sqrt{s} = 0.9$ TeV: track characteristics for experimental data (left) and default simulation (right) before (histogram) and after (points) the track-quality requirements described in the text. Top row: track pseudorapidity; center row: track transverse momentum; bottom row: track impact parameter.

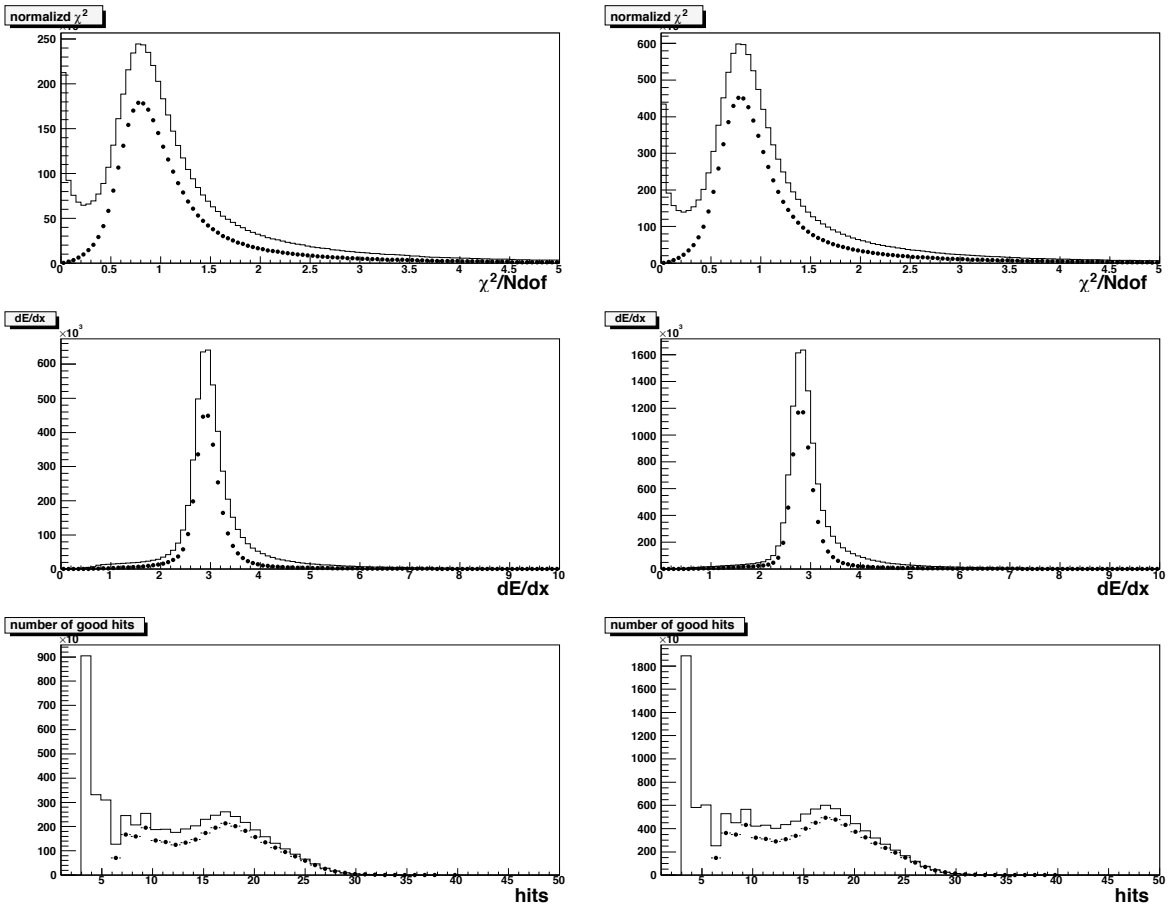

Figure 2: Events at $\sqrt{s} = 0.9$ TeV: track characteristics for data (left) and default simulation (right) before (histogram) and after (points) the track quality requirements described in the text. Top row: track χ^2 per degree of freedom; center row: track dE/dx (in MeV/cm); bottom row: number of valid hits per track.

4 Definition of Signal Sample and Coulomb Corrections

We form pairs of same-charge tracks passing the selection described in Sec. 2 and proceed to construct their Q-value distribution, as described in Sec. 1. We use for our measurements all the events with a value of Q in the range $0.02 < Q < 2$ GeV. The upper limit is chosen in such a way as to provide a wide-enough side band for the normalization of the reference sample; the lower limit is instead chosen to ensure a stable reconstruction efficiency in the studied kinematical region to pairs of track with very similar geometrical and kinematical parameters.

Since in this analysis the Q value distribution has to be normalized to a reference sample, the track reconstruction efficiency is not a relevant issue. What is relevant is rather the ratio of the efficiencies on the signal pairs and on the reference samples of track pairs used for the measurement. This is shown in a sample of simulated events in Fig. 3. The tracking efficiency ratio is observed to be quite flat as a function of Q-value in the region above $Q > 0.02$ GeV.

Pairs of charged tracks close in phase space are known to be subjected to a Coulomb interaction which modifies the two-particle relative momentum distribution in a different way for same-charge (S) and different-charge (D) pairs. The Coulomb effect is parametrized in the literature

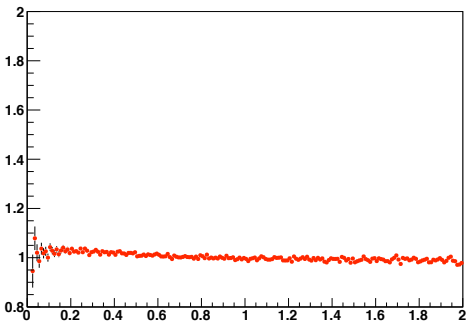

Figure 3: Distribution of the ratio of track-pair reconstruction efficiency for the signal sample and a reference sample obtained as decribed in the text (Sec. 5), as a function of the pair Q-value.

by the Gamow factors [15]

$$W_S(\eta) = \frac{e^{2\pi\eta} - 1}{2\pi\eta}, \quad W_D(\eta) = \frac{1 - e^{-2\pi\eta}}{2\pi\eta}$$

with $\eta = \alpha m_\pi / Q$.

The effect of a Coulomb interaction is visible in Fig. 4, where the ratio between the Q-value of different-charge particles in experimental data and in simulated events (which do not contain a Coulomb effect) is shown and compared with the inverse of the W_D factor. The right panel in Fig. 4 shows the same ratio after the data is corrected by applying the Gamow factor W_D. The good agreement between data and simulation observed after the correction is applied to opposite-charge pairs gives us confidence in the application of the Coulomb correction also to same-charge pairs.

$\pi^\pm\pi^\pm$

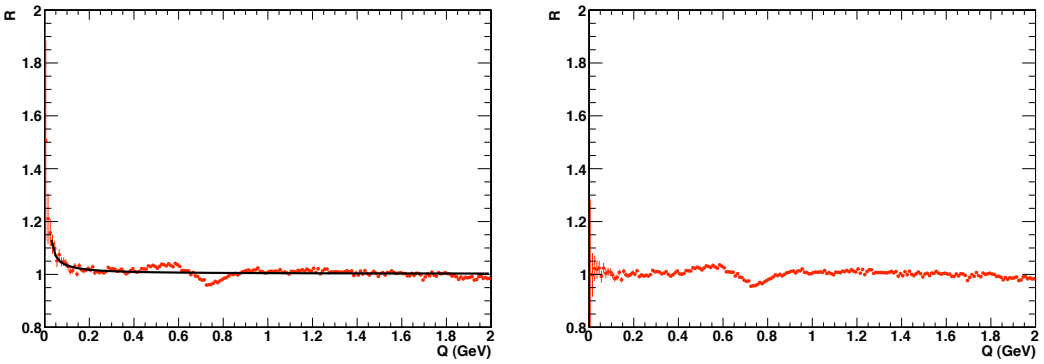

$\pi^\pm\pi^\mp$

Figure 4: Left: Distribution of the R ratio between the Q-value of different-charge particle pairs in data and different-charge candidates in simulated events. The simulation does not include such Coulomb effect. The line corresponds to the inverse of the Gamow factor W_D. Right: the same ratio after data are corrected by applying the Gamow factor W_D to the ratio R.

5 Reference Samples

We considered several methods to combine uncorrelated charged tracks into pairs to define a reference sample representing the denominator in eq. 1.

1. *Different-Charge Particles.* This data set is the most natural choice but it presents some drawbacks. Different-charge pairs contain several resonances which are not present in same-charge combinations. Furthermore, we point out here a fact which went unnoticed in most of the analyses from older experiments: quantum field theory predicts that also different-charge tracks may undergo Bose–Einstein correlations [16–19], as a consequence of virtual processes involving the ρ and higher-mass common states.

   The Q-value distribution of the ratio R between same-sign and different-sign track pairs is shown in Fig. 5(a).

2. *Opposite-Hemisphere Particles.* We combine tracks by inverting in space the three-momentum of only one of the two particles, computing $Q_O = -(p_1 - p_2^o)$, where $p_2^o = (E_2, -\vec{p}_2)$. Tracks produced in opposite hemispheres populate the low-Q-value region of this "inverted-momentum" sample. They constitute our default reference sample. The Q-value distribution of the ratio R between same-charge track pairs and inverted-momentum same-charge pairs is shown in Fig. 5(b) for data and default simulation. A clear enhancement for low Q-values is evident. The same effect is not present in the equivalent distribution extracted from the default simulation. This fortifies our hypothesis that the low-Q-value enhancement is due to the Bose–Einstein correlation effect. The procedure described above can also be applied to pairs of particles with different charge. This is shown in Fig. 5(c).

3. *Rotated Particles.* We produce a statistically-independent reference sample with another spatial trasformation of the track parameters. We invert the value of the x and y components of the three-momentum of one of the two particles, leaving the other particle unchanged. Figure 5(d) shows the R distribution for 0.9 TeV data and default simulation obtained this way.

4. *Mixing Events.* We form this sample by combining tracks from different events. We have investigated three alternative ways to choose events providing the tracks to be paired with the one under consideration. The first way (a) consists in choosing events at random from the data sample. The second (b) is to combine tracks taken from events with similar track density; for this purpose, we consider three η bins ($-2.4 < \eta < -0.8$, $|\eta| < 0.8$, and $0.8 < \eta < 2.4$), and we combine events with the three values of charged track density per η bin, $dN/d\eta$, differing by no more than 20%. As a third criterion (c), we compute the invariant mass from all the tracks in each event, $\mathcal{M} = (\Sigma_i p_i)^2$, and pair-up events if the difference in $\mathcal{M}$ is less than 20%. Each used event is combined with one and only one other event in the dataset. The results from this approach are displayed in Fig. 6.

5. *Non-Identical Particles.* The measured ionization-energy loss in the tracking detector can be used to separate pions from kaons and proton candidates. We may extract a reference sample by combining a track identified as a pion with another one failing pion identification. Figure 7 shows the R distribution for 0.9 TeV data and default simulation obtained this way.

   In this case, the shape of the ratio is not an horizontal straight line in the high-Q region because of a kinematical distortion, which is almost perfectly reproduced by the simulation; the distortion originates from the fact that, in the control sample, a π is combined with a particle which has almost always $p < 1.5$ GeV/c. For this reason, and due to the smaller statistics of this comparison, this sample is not used as a reference in the computation of a systematic error.

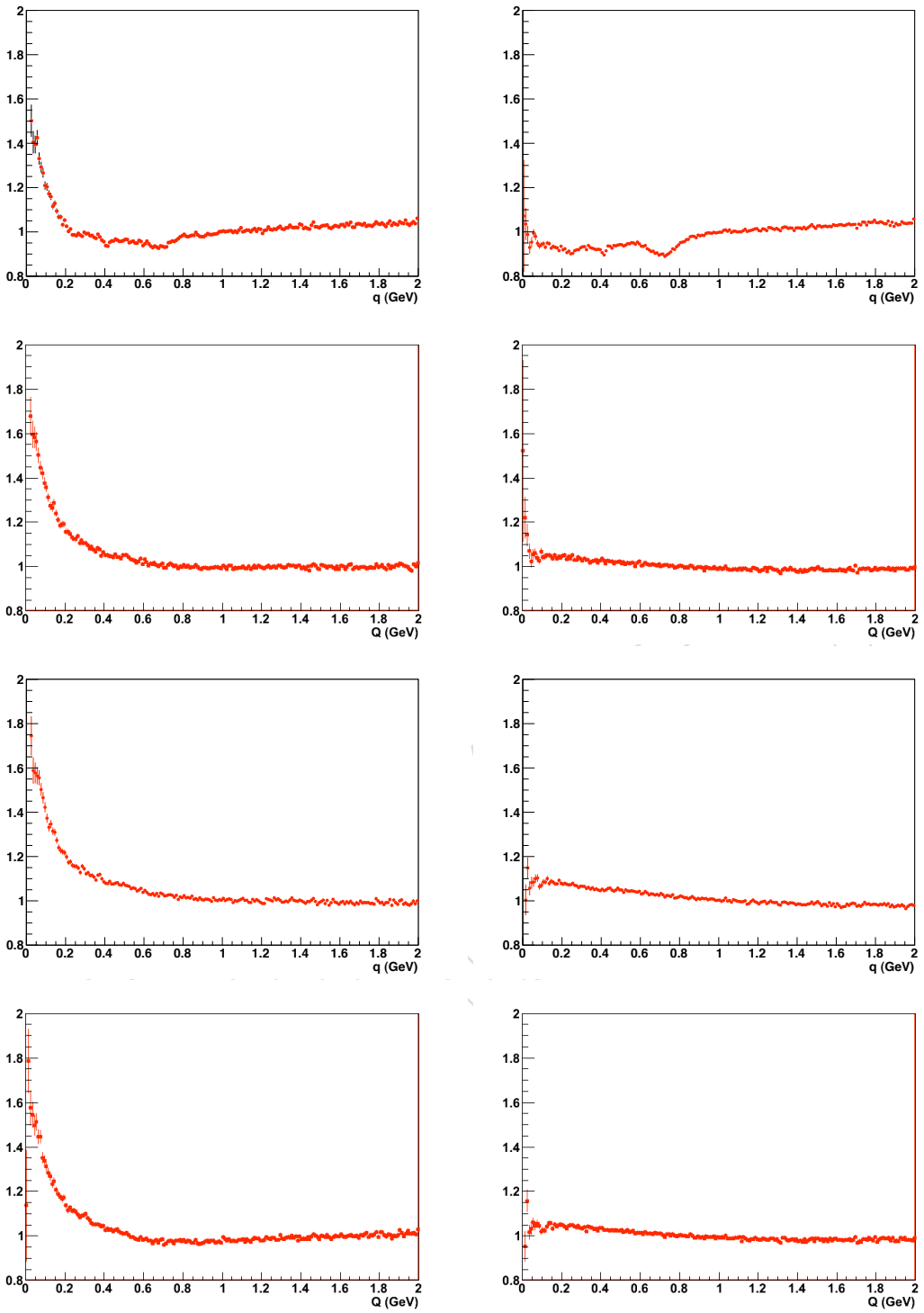

Figure 5: (a) Distribution of the R ratio between the Q-value of same-charge and different-charge particles in 0.9 TeV events. (b) Distribution of the R ratio between the Q-value of same-charge pairs and same-charge pairs where one of the two particles has its three-momentum inverted. (c) Distribution of the R ratio between the Q-value of same-charge pairs and different-charge pairs where one of the two particles has its three-momentum inverted. (d) Distribution of the R ratio between the Q-value of same-charge pairs and same-charge pairs where we invert the track direction of one of the two tracks in the transverse plane. The left figures show experimental data, the right figures show the default simulation.

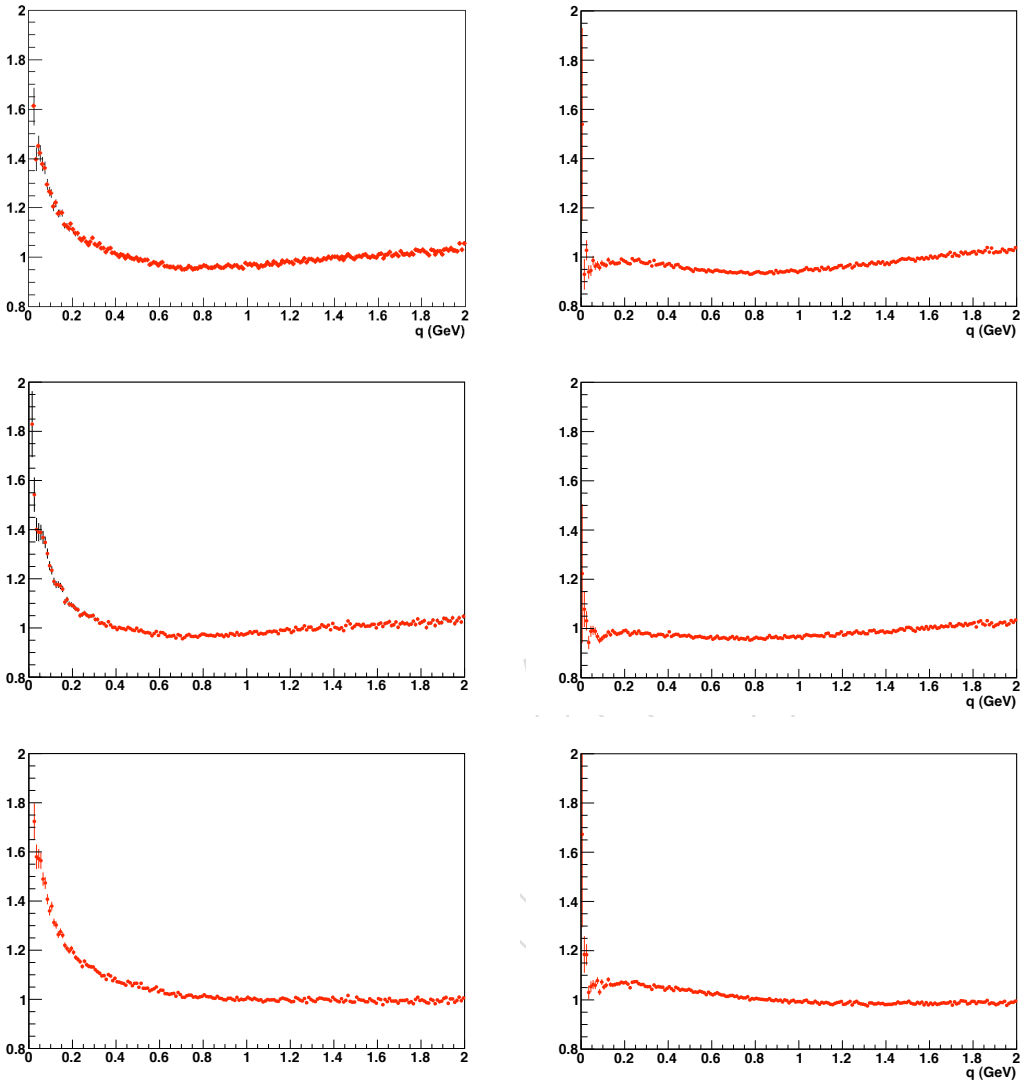

Figure 6: (a) Distribution of the R ratio between the Q-value of same-charge particle pairs and same-charge pairs where the two particles belong to different events selected at random. (b) Distribution of the R-ratio between the Q-value of same-charge pairs and same-charge pairs where the two particles belong to different events with similar track density. (c) Distribution of the R-ratio between the Q-value of same-charge pairs and same-charge pairs where the two particles belong to events with similar total track invariant mass. The left figures show 0.9 TeV collisions data, the right figures show the corresponding default simulation. See the text for more details.

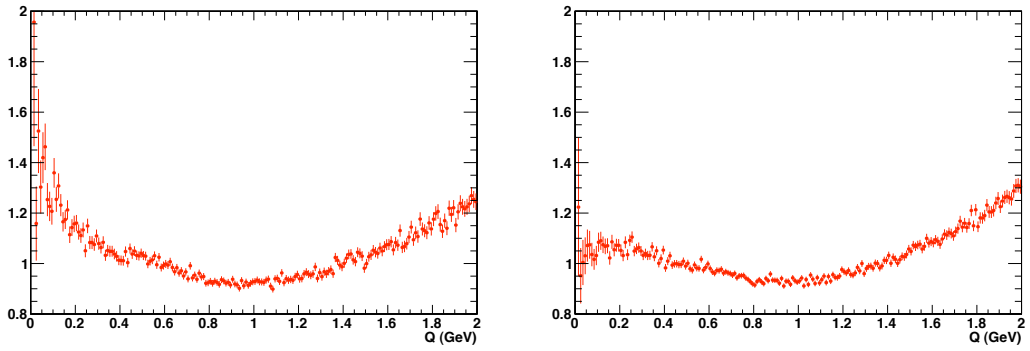

Figure 7: Left: Distribution of the R ratio between the Q-value of same-charge pion candidates and same-charge candidates having different identity (one π candidate and one non-π candidate). Right: same, on 0.9 TeV default simulation.

6 Determination of Bose–Einstein Correlation Parameters

As discussed in Sec. 1, a phenomenologically-motivated form for the functional dependence of the R ratio on two-particle Q-value involves four parameters: the normalization C, the quantity λ, the form $\Omega(Qr)$, and the δ parameter. Alternative functions are also tried to study the compatibility with CMS data. We use as our default parametrization the one of eq. 2 with $\Omega(Qr) = e^{-Qr}$.

In order to remove as much as possible the biases due the particular construction of the reference samples, it appears favourable to create, for each reference sample, a double ratio $\mathcal{R}$ constructed as follows:

$$\mathrm{R} = \mathrm{R} \;/\; \mathrm{R}_{MC} = \frac{\frac{dN/dQ}{dN/dQ_{ref}}}{\frac{dN/dQ_{MC}}{dN/dQ_{MC,ref}}} \tag{4}$$

where Q_{MC} and $Q_{MC,ref}$ are the Q-values extracted from the default simulation, which as stated above does not include a modeling of Bose–Einstein correlations.

The results of fits to the double ratios $\mathcal{R}$ are shown in Fig. 8 and 9, and they and reported in table 2.

Table 2: Results of χ^2 fits to the double ratio $\mathcal{R}$ with different definitions of the reference sample using the exponential function. The last line shows the result obtained by combining all the reference samples as described in section 8

Reference Sample	p-value	C	λ	r (fm)	δ
Different charge (1)	2.19×10^{-1}	1.005 ± 0.003	0.557 ± 0.025	1.457 ± 0.064	$(-3.51 \pm 2.37) \times 10^{-3}$
Opposite Hemisphere (2)	7.30×10^{-2}	0.995 ± 0.003	0.633 ± 0.027	1.497 ± 0.056	$1.07 \pm 0.20 \times 10^{-2}$
Opposite Hem. from DS (2a)	1.19×10^{-1}	0.989 ± 0.003	0.591 ± 0.025	1.417 ± 0.056	$1.32 \pm 0.21 \times 10^{-2}$
Rotated (3)	2.42×10^{-4}	0.930 ± 0.003	0.677 ± 0.022	1.290 ± 0.039	$5.79 \pm 0.24 \times 10^{-2}$
Event Mix (4a) (random order)	2.11×10^{-2}	1.040 ± 0.002	0.649 ± 0.032	1.893 ± 0.072	$-1.85 \pm 0.15 \times 10^{-2}$
Event Mix (4b) ($dN/d\eta$)	4.51×10^{-2}	1.012 ± 0.002	0.641 ± 0.030	1.799 ± 0.066	$-1.28 \pm 1.61 \times 10^{-3}$
Event Mix (4c) ($\mathcal{M}$)	5.19×10^{-3}	1.005 ± 0.002	0.670 ± 0.027	1.749 ± 0.057	$2.50 \pm 1.53 \times 10^{-3}$
Combined Result	1.76×10^{-2}	1.001 ± 0.002	0.634 ± 0.021	1.620 ± 0.046	$4.75 \pm 1.39 \times 10^{-3}$

A large correlation is found between λ and r, and between δ and C, as shown in table 3, which reports the correlation coefficients for the values obtained with the Opposite-Hemisphere reference sample (similar values are obtained in all other cases).

Table 3: Correlation coefficients for the fit parameters obtained with the Opposite-Hemisphere reference sample.

	C	λ	r	δ
C	1			
λ	0.33	1		
r	0.68	0.83	1	
δ	-0.96	-0.28	-0.614	1

In order to test the agreement of different functional parametrizations of the Bose–Einstein correlation with our data, we further fit the double ratio $\mathcal{R}$ obtained with the Opposite-Hemisphere reference sample (2) using three alternative forms: a Gaussian form $\Omega(Qr) = e^{-(Qr)^2}$ in eq. 2,

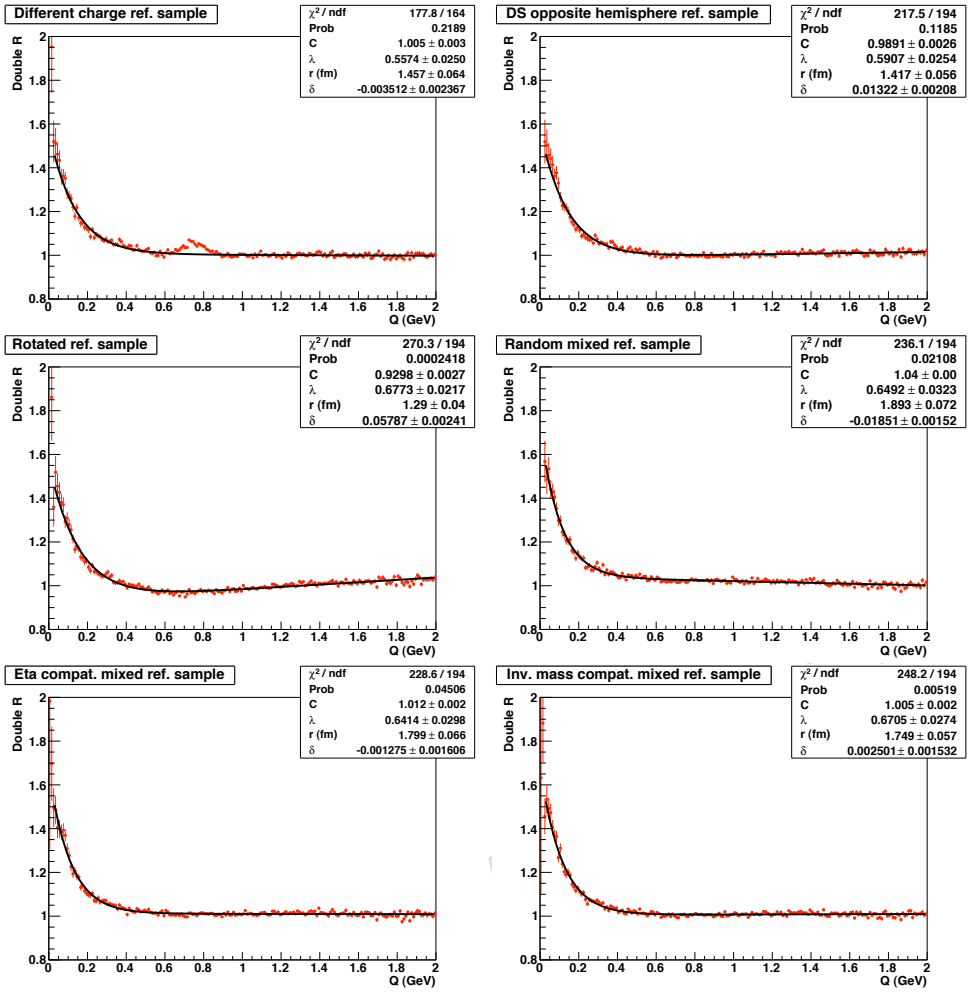

Figure 8: Distribution of the double ratio $\mathcal{R}$ defined as in eq. 4, for different reference samples. Top left: different-sign candidates (range $0.6 < Q < 0.9GeV$ excluded in the fit). Top right: same-charge pairs and different-charge pairs where one of the two particles in the pairs has its three-momentum inverted. Center left: same-charge candidates where we invert the x and y components of the three-momentum of one of the two particles. Center right: same-charge pairs where the two particles belong to different events selected at random. Bottom left: same-charge pairs where the two particles belong to different events of similar track density. Bottom right: same-charge pairs where the two particles belong to different events with similar value of total invariant mass of all tracks.

which is widely used by other experiments to fit their signal; the exponential form $\Omega(Qr) = e^{-Qr}$; and a Gaussian form in eq. 3. From the fit quality it is evident that the exponential hypothesis reproduces our data much better than the Gaussian ones. The fact that a Gaussian shape is not a good representation of experimental data could be envisaged also in previous papers (see, *e.g.*, the analysis of ALEPH data described in [12]). Hence we choose to quote the parameters obtained from an exponential shape fit.

As a cross-check, we present also the double ratio for an enriched sample of $\pi\pi$ pairs, and for pairs where one particle is tagged as a π and the other as a non-π (see Fig. 10); the fact that the latter distribution is essentially flat clearly confirms our interpretation that the low-Q peak is produced by a Bose–Einstein correlation effect.

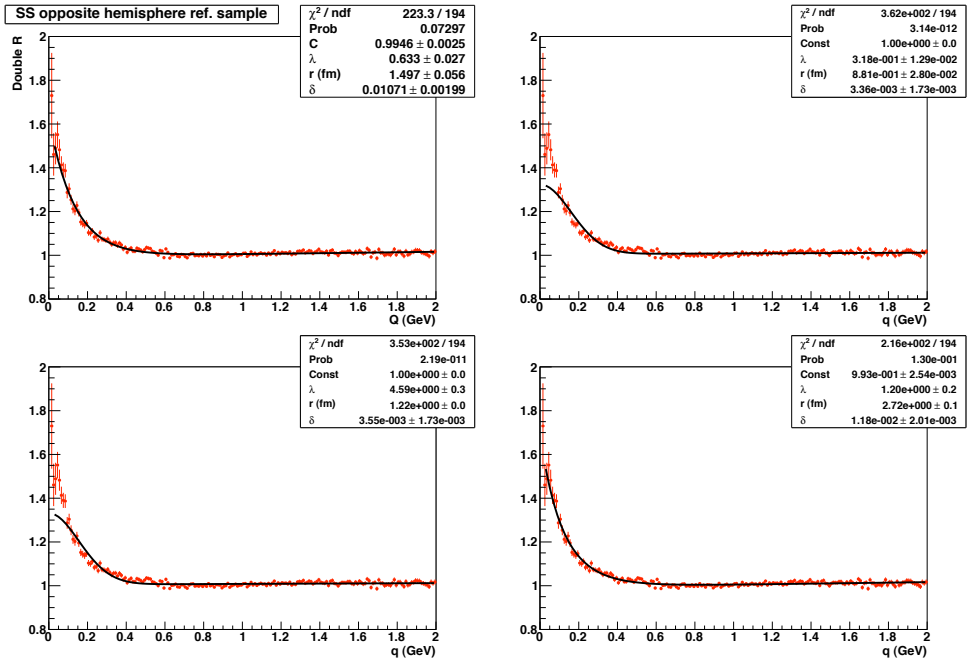

Figure 9: Distribution of the double ratio $\mathcal{R}$ between the Q-value of same-charge pairs and same-charge pairs where one of the two particles in the pair has its three-momentum inverted. Top left: fit with an exponential function (eq. 2 with $\Omega(Qr) = e^{-Qr}$). Top right: fit with a Gaussian function (eq. 2 with $\Omega(Qr) = e^{-(Qr)^2}$). Bottom left: fit with a Kozlov-Gaussian function (eq. 3 with $\Omega(Qr) = e^{-(Qr)^2}$). Bottom right: fit with Kozlov-exponential function (eq. 3 $\Omega(Qr) = e^{-Qr}$).

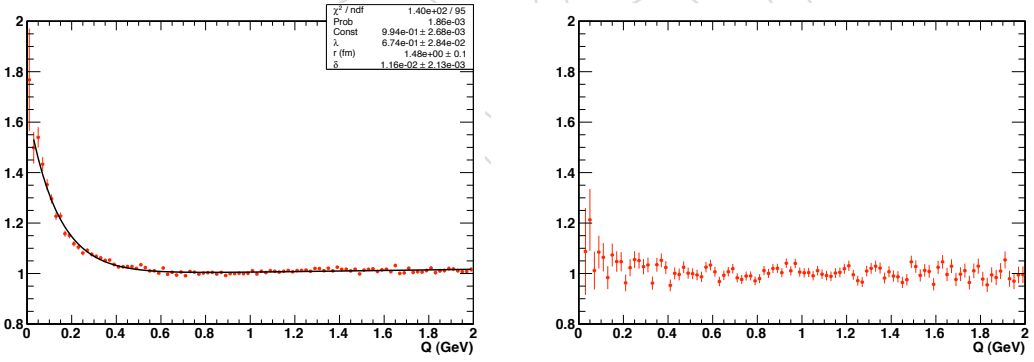

Figure 10: Distribution of the double ratio $\mathcal{R}$ between the Q-value of same-charge particles and a reference sample where one of the two has its three-momentum inverted, data over simulation. Left: same-sign positively identified pion candidates (with Coulomb correction). Right: same-sign pion and not-pion identified candidates (without Coulomb correction).

For the data collected at $\sqrt{s} = 2.36$ TeV, given the limited statistics only the results obtained with the Opposite-Hemisphere-Particle (2) reference sample are presented here. The double ratio $\mathcal{R}$, which is now constructed with 2.36 TeV default simulated events at the denominator, is shown in Fig. 11. The fit is obtained with an exponential function (eq. 2 with $\Omega(Qr) = e^{-Qr}$) and results are reported in table 4. An evidence of Bose-Einstein correlations is clear also in data collected at this never-reached-before energy.

Table 4: Fit results to the double ratio $\mathcal{R}$ for 2.36 TeV data.

Reference Sample	p-value	C	λ	r (fm)	δ
Opposite Hemisphere (2)	3.39×10^{-1}	0.991±0.006	0.68±0.11	1.96±0.20	$(1.47 \pm 0.48) \times 10^{-2}$

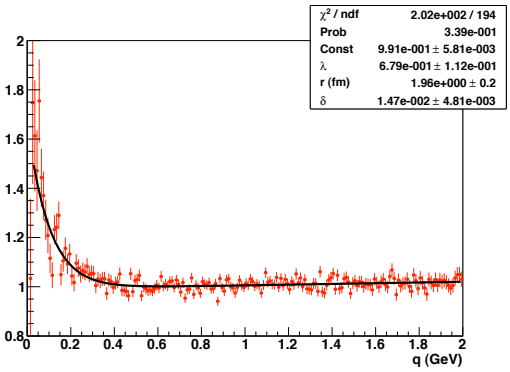

Figure 11: Distribution of the double ratio $\mathcal{R}$ between the Q-value of same-charge pairs for data taken at 2.36 TeV and same-charge pairs where one of the two particles in the pair has its three-momentum inverted. The fit is obtained with an exponential function (eq. 2 with $\Omega(Qr) = e^{-Qr}$).

7 Dependence of Bose–Einstein Correlations on Pair Kinematics

We perform a study of the dependence of the Bose–Einstein correlation signal in the $\mathcal{R}$ distribution on various particle and event observables. In the following the behavior of the parameters λ and r extracted by the exponential fit (eq. 2) to $\mathcal{R}$ are shown together with their statistical errors. The dependence on tracks mean p_t is shown in Fig. 12, the one on track pseudorapidity η in Fig. 13, and the one on the energy difference between the particles in a pair, $Q_0 = |E_i - E_j|$, in Fig. 14. Finally, Fig. 15 shows the dependence on the charged multiplicity in the event.

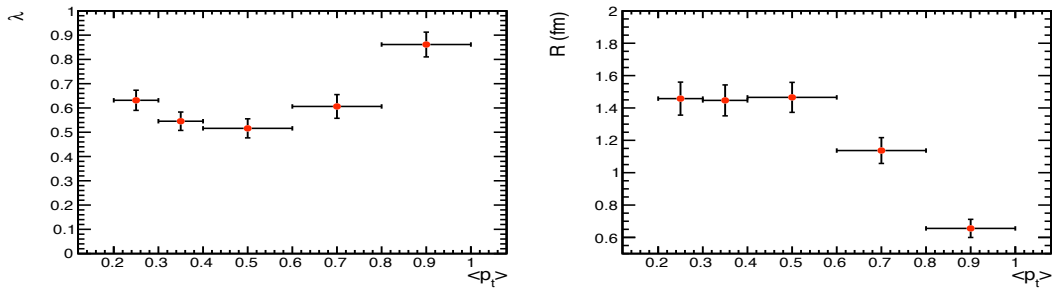

Figure 12: Dependence of fit parameters λ and r on track mean p_t.

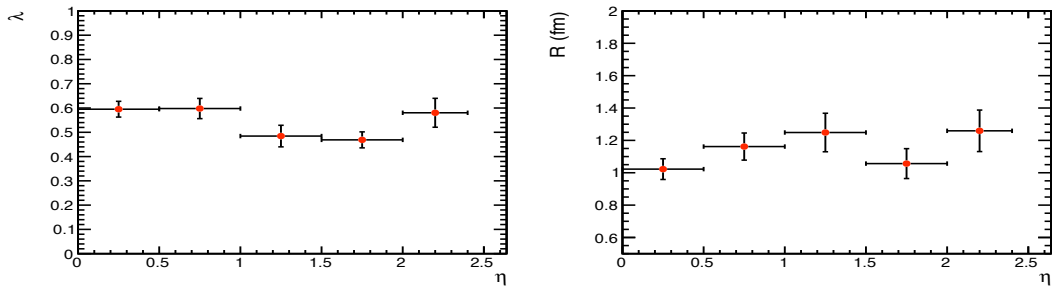

Figure 13: Dependence of fit parameters λ and r on track pseudorapidity.

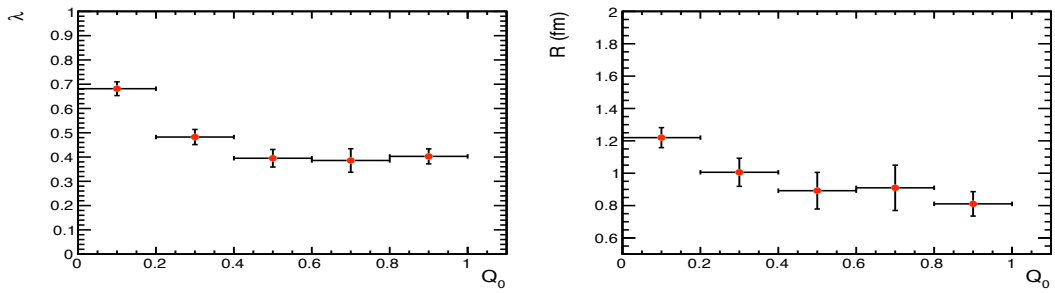

Figure 14: Dependence of fit parameters λ and r on track energy difference Q_0.

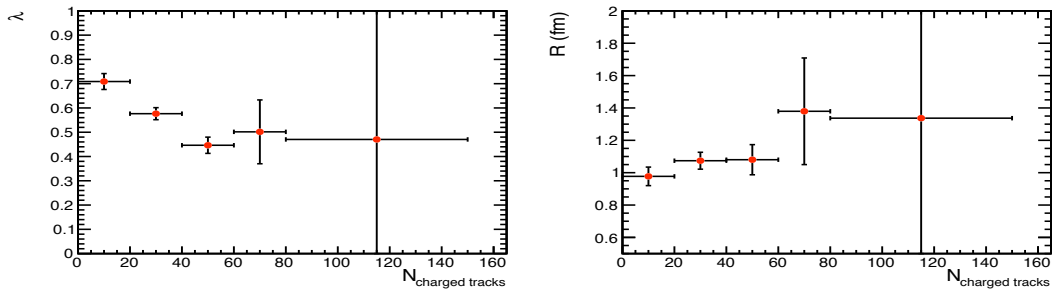

Figure 15: Dependence of fit parameters λ and r on event charged-track multiplicity.

8 Combined Results and Systematic Uncertainties

The experimental technique of taking a double ratio $\mathcal{R}$ between data and simulation to determine the parameters of the Bose–Einstein correlation effect reduces considerably the sources of bias due to track inefficiency and other detector-related effects. Still, a sizeable spread in the parameters governing the strength and size of the emission region can be observed in the measurements obtained with different reference samples. As any of these samples may introduce not easily-predictable biases, none of them is *a priori* preferable. As a consequence, in the literature experiments often report several results obtained with different reference samples. In our case this is done in table 2.

However we consider valuable to provide a single value for each of the fit parameters, together with an estimate of the systematic error connected with the choice of the reference. We follow an approach here which satisfies the following requirements:

- it deals parithetically with the plethora of used reference samples;
- it accounts properly (and easily) for the statistical correlations between the different measurements, all sharing the same signal, but differing in the composition of the reference sample;
- it allows an easy and well-defined estimate of the systematic uncertainty related to the choice of the reference sample.

For this purpose, we compute a new reference sample as the average of the $m = 7$ sets described in Sec. 6 and listed in table 2:

$$\mathrm{R}^{avg} = \frac{dN/dQ}{dN/dQ_{MC}} \left(\frac{1}{m} \sum_{i=1}^{m} \frac{dN/dQ^{i}_{MC}}{dN/dQ^{i}} \right). \tag{5}$$

$\mathcal{R}^{avg}$ is fit with the exponential form to determine the Bose–Einstein correlation parameters. Results are displayed in Fig. 16, while the returned values of the parameters are found in the last line of table 2.

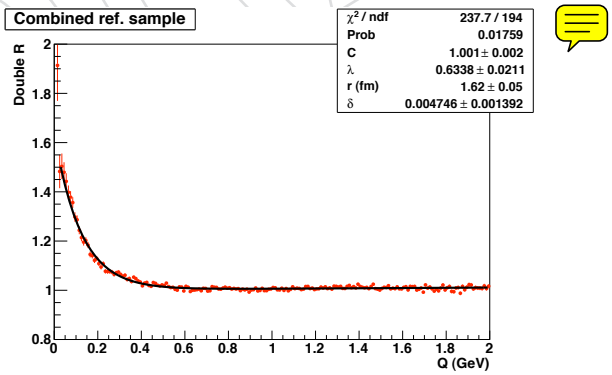

Figure 16: Results of the exponential fit to $\mathcal{R}^{avg}$ when combining all the reference samples, for 0.9 TeV collisions.

We choose to estimate as a systematic uncertainty to each parameter the RMS spread of the results obtained with the seven different reference samples.

An uncertainty due to the bias introduced by track selection requirements may be estimated with the help of the simulation generated with Bose–Einstein effects modeled with an expo-

nential functional form. By comparing the results obtained using reconstructed tracks in that simulation to those obtained using generated charged particles, the bias is found negligible ($\pm$0.8%) for λ, while it is more significant ($\pm$10.3%) for r.

Other sources of systematic uncertainty, such as Coulomb corrections, choice of fit range, variations in the track selection requirements, all yield a negligible effect on λ and r.

The total systematic uncertainty is computed as the quadratic sum of the one arising from the variation of reference samples and the one due to a reconstruction bias. The two parameters are estimated to be $r = 1.62 \pm 0.05$ (stat) $\pm$0.27(syst) fm and $\lambda = 0.634 \pm 0.021$ (stat) $\pm$0.047 (syst) in 0.9 TeV collisions. Concerning 2.36 TeV data, we quote the same estimates of systematic uncertanty on the two parameters obtained from the analysis of 0.9 TeV collisions. The estimates are $r = 1.96 \pm 0.20$ (stat) $\pm$0.27 (syst) fm, and $\lambda = 0.68 \pm 0.11$ (stat) $\pm$0.05 (syst).

9 Conclusions

A signal of Bose–Einstein correlations has been extracted from pairs of same-charge particles measured by the CMS tracking system in 0.9 and 2.36 TeV proton-proton collision data delivered by the Large Hadron Collider in December 2009. The signal is well modeled by the functional form proposed in [12], whose parameters determine the strength of the interference effect and the size of the emission region.

At 0.9 TeV we measure $r = 1.62 \pm 0.05$ (stat) $\pm$0.27(syst) fm and $\lambda = 0.634 \pm 0.021$ (stat) $\pm$0.047 (syst); at 2.36 TeV we measure $r = 1.96 \pm 0.20$ (stat) $\pm$0.27 (syst) fm, and $\lambda = 0.68 \pm 0.11$ (stat) $\pm$0.05 (syst). The quoted systematic uncertainties result from the choice of the reference sample and from the estimate of a reconstruction bias.

The dependence of the measured values of r and λ on track momentum and local charged particle density evidence a decrease of the size of the emission region with track momentum; other effects are found to be less significant.

10 Acknowledgements

We wish to thank Torbjorn Sjöstrand for his assistance with the generation of Monte Carlo samples simulated with Pythia by including the effect of Bose–Einstein correlations. We also thank Andrea Giammanco for useful discussions concerning the use of track energy loss measurements.

References

[1] CMS Collaboration, "The CMS experiment at the CERN LHC", *JINST* **0803:S08004** (2008).

[2] G. Goldhaber et al. *Phys. Rev.* **120** (1960) 300.

[3] I. Juricic et al. *Phys. Rev.* **D39** (1989) 1.

[4] M. Althoff et al. *Z. Phys.* **C30** (1986) 355.

[5] ALEPH Collaboration *Eur. Phys. J.* **C36** (2004) 147.

[6] E. Torassa, "Soft hadron phenomena at LEP", *HEP 93 Proceedings, Ed. by J. Carr and M. Perrottet* (1993) 602.

[7] OPAL Collaboration *Phys. Lett.* **B559** (2003) 131.

[8] M. Adamus et al. *Z. Phys.* **C37** (1988) 347.

[9] M. Derrick *Acta Phys. Polon.* **B33** (2002) 3281.

[10] C. Albajar et al. *Phys. Lett.* **B226** (1989) 410.

[11] G.A. Kozlov, O. Utyuzh, G. Wilk, and Z. Wlodarczyk, "Some forgotten features of Bose-Einstein Correlations", *Presented at Relativistic Nuclear Physics: from Nuclotron to LHC energies* **hep-ph/07103710**.

[12] G.A. Kozlov, L. Lovas, S. Tokar, Yu.A. Boudagov and A.N. Sissakian, "Bose-Einstein correlations at LEP and Tevatron energies", *Rev. Mod. Phys.* **hep-ph/0510027**.

[13] S. M. T. Sjostrand and P. Skands, "PYTHIA 6.4 physics and manual", *JHEP05(2006)26* (2006).

[14] T. Sjostrand. private communication.

[15] M. Gyulassy, S. Kaufmann, and L. W. Wilson *Phys. Rev.* **C20** (1979) 2267.

[16] I. V. Andreev, M. Plmer, and R. M. Weiner *Phys. Rev. Lett.* **67** (1991) 3475.

[17] L. V. Razumov and R. M. Weiner *Phys. Lett. B* **348** (1995) 133.

[18] M. Bowler *Phys. Lett. B* **276** (1992) 237.

[19] R. M. Weiner *Physics Reports* **327** (2000) 249.